



## **Targeting CXCR4 (CXC Chemokine Receptor Type 4) for Molecular Imaging of Aldosterone-Producing Adenoma**

Heinze, Britta ; Fuss, Carmina T ; Mulatero, Paolo ; Beuschlein, Felix ; Reincke, Martin ; Mustafa, Mona ; Schirbel, Andreas ; Deutschbein, Timo ; Williams, Tracy Ann ; Rhayem, Yara ; Quinkler, Marcus ; Rayes, Nada ; Monticone, Silvia ; Wild, Vanessa ; Gomez-Sanchez, Celso E ; Reis, Anna-Carinna ; Petersenn, Stephan ; Wester, Hans-Juergen ; Kropf, Saskia ; Fassnacht, Martin ; Lang, Katharina ; Herrmann, Ken ; Buck, Andreas K ; Bluemel, Christina ; Hahner, Stefanie

**Abstract:** Primary aldosteronism is the most frequent cause of secondary hypertension and is associated with increased morbidity and mortality compared with hypertensive controls. The central diagnostic challenge is the differentiation between bilateral and unilateral disease, which determines treatment options. Bilateral adrenal venous sampling, currently recommended for differential diagnosis, is an invasive procedure with several drawbacks, making it desirable to develop novel noninvasive diagnostic tools. When investigating the expression pattern of chemokine receptors by quantitative real-time polymerase chain reaction and immunohistochemistry, we observed high expression of CXCR4 (CXC chemokine receptor type 4) in aldosterone-producing tissue in normal adrenals, adjacent adrenal cortex from adrenocortical adenomas, and in aldosterone-producing adenomas (APA), correlating strongly with the expression of CYP11B2 (aldosterone synthase). In contrast, CXCR4 was not detected in the majority of nonfunctioning adenomas that are frequently found coincidentally. The specific CXCR4 ligand <sup>68</sup>Ga-pentixafor has recently been established as radiotracer for molecular imaging of CXCR4 expression and showed strong and specific binding to cryosections of APAs in our study. We further investigated 9 patients with primary aldosteronism because of APA by <sup>68</sup>Ga-pentixafor-positron emission tomography. The tracer uptake was significantly higher on the side of increased adrenocortical aldosterone secretion in patients with APAs compared with patients investigated by <sup>68</sup>Ga-pentixafor-positron emission tomography for other causes. Molecular imaging of aldosterone-producing tissue by a CXCR4-specific ligand may, therefore, be a highly promising tool for noninvasive characterization of patients with APAs.

DOI: <https://doi.org/10.1161/HYPERTENSIONAHA.117.09975>

Posted at the Zurich Open Repository and Archive, University of Zurich

ZORA URL: <https://doi.org/10.5167/uzh-145897>

Journal Article

Published Version

Originally published at:

Heinze, Britta; Fuss, Carmina T; Mulatero, Paolo; Beuschlein, Felix; Reincke, Martin; Mustafa, Mona; Schirbel, Andreas; Deutschbein, Timo; Williams, Tracy Ann; Rhayem, Yara; Quinkler, Marcus; Rayes, Nada; Monticone, Silvia; Wild, Vanessa; Gomez-Sanchez, Celso E; Reis, Anna-Carinna; Petersenn, Stephan; Wester, Hans-Juergen; Kropf, Saskia; Fassnacht, Martin; Lang, Katharina; Herrmann, Ken;

Buck, Andreas K; Bluemel, Christina; Hahner, Stefanie (2018). Targeting CXCR4 (CXC Chemokine Receptor Type 4) for Molecular Imaging of Aldosterone-Producing Adenoma. *Hypertension*, 71(2):317-325. DOI: <https://doi.org/10.1161/HYPERTENSIONAHA.117.09975>

## Targeting CXCR4 (CXC Chemokine Receptor Type 4) for Molecular Imaging of Aldosterone-Producing Adenoma

Britta Heinze,\* Carmina T. Fuss,\* Paolo Mulatero, Felix Beuschlein, Martin Reincke, Mona Mustafa, Andreas Schirbel, Timo Deutschbein, Tracy Ann Williams, Yara Rhayem, Marcus Quinkler, Nada Rayes, Silvia Monticone, Vanessa Wild, Celso E. Gomez-Sanchez, Anna-Carina Reis, Stephan Petersenn, Hans-Juergen Wester, Saskia Kropf, Martin Fassnacht, Katharina Lang, Ken Herrmann, Andreas K. Buck, Christina Bluemel, Stefanie Hahner

**Abstract**—Primary aldosteronism is the most frequent cause of secondary hypertension and is associated with increased morbidity and mortality compared with hypertensive controls. The central diagnostic challenge is the differentiation between bilateral and unilateral disease, which determines treatment options. Bilateral adrenal venous sampling, currently recommended for differential diagnosis, is an invasive procedure with several drawbacks, making it desirable to develop novel noninvasive diagnostic tools. When investigating the expression pattern of chemokine receptors by quantitative real-time polymerase chain reaction and immunohistochemistry, we observed high expression of CXCR4 (CXC chemokine receptor type 4) in aldosterone-producing tissue in normal adrenals, adjacent adrenal cortex from adrenocortical adenomas, and in aldosterone-producing adenomas (APA), correlating strongly with the expression of CYP11B2 (aldosterone synthase). In contrast, CXCR4 was not detected in the majority of nonfunctioning adenomas that are frequently found coincidentally. The specific CXCR4 ligand <sup>68</sup>Ga-pentixafor has recently been established as radiotracer for molecular imaging of CXCR4 expression and showed strong and specific binding to cryosections of APAs in our study. We further investigated 9 patients with primary aldosteronism because of APA by <sup>68</sup>Ga-pentixafor–positron emission tomography. The tracer uptake was significantly higher on the side of increased adrenocortical aldosterone secretion in patients with APAs compared with patients investigated by <sup>68</sup>Ga-pentixafor–positron emission tomography for other causes. Molecular imaging of aldosterone-producing tissue by a CXCR4-specific ligand may, therefore, be a highly promising tool for noninvasive characterization of patients with APAs. (*Hypertension*. 2018;71:317-325. DOI: 10.1161/HYPERTENSIONAHA.117.09975.) • [Online Data Supplement](#)

**Key Words:** adrenal cortex ■ aldosterone ■ Ga68-pentixafor ■ humans ■ molecular imaging

Primary aldosteronism (PA) is characterized by adrenocortical oversecretion of aldosterone, which causes increased cardiovascular and metabolic morbidity.<sup>1-4</sup> In most cases, PA is either caused by bilateral adrenal hyperplasia or unilateral aldosterone-producing adenoma (APA).<sup>5</sup> Swift and thorough diagnostic evaluation is of high importance for further therapeutic decision-making: although APA may be cured by surgery, therapy of bilateral adrenal hyperplasia consists of life-long treatment with mineralocorticoid receptor

antagonists.<sup>6</sup> Conventional imaging reveals adrenal lesions with an age-dependent increase and an overall prevalence of 2% to 10%, mainly representing nonfunctioning adenomas (NFAs).<sup>7</sup> Thus, NFA coincident with biochemical PA may be falsely interpreted as APA instead of bilateral adrenal hyperplasia, potentially leading to avoidable surgical interventions. Accordingly, conventional imaging methods still do not allow for an unequivocal differential diagnosis in patients with PA.<sup>8-10</sup> Adrenal vein sampling (AVS) has, therefore, remained

Received July 15, 2017; first decision July 25, 2017; revision accepted November 28, 2017.

From the Department of Internal Medicine I, Endocrinology and Diabetes Unit (B.H., C.T.F., M.F., K.L., S.H.), Department of Nuclear Medicine (A.S., K.H., A.K.B., C.B.), and Comprehensive Cancer Center Wuerzburg (T.D., M.F.), University Hospital of Wuerzburg, University of Wuerzburg, Germany; Division of Internal Medicine and Hypertension, Department of Medical Sciences, University of Torino, Italy (P.M., T.A.W., S.M.); Medizinische Klinik und Poliklinik IV, Klinikum der Universität München, Germany (F.B., M.R., T.A.W., Y.R.); Department of Nuclear Medicine, Klinikum rechts der Isar der Technischen Universität München, Germany (M.M.); Endocrinology in Charlottenburg, Berlin, Germany (M.Q.); Department of General, Visceral, and Transplant Surgery, Campus Virchow Klinikum, Charité–Universitätsmedizin Berlin, Germany (N.R.); Department of Pathology, University of Würzburg, Germany (V.W.); Division of Endocrinology, G.V. (Sonny) Montgomery VA Medical Center, MS (C.E.G.-S.); Institute of Pathology, University Hospital Essen, University of Duisburg-Essen, Germany (A.-C.R.); ENDOC, Center for Endocrine Tumors, Hamburg, Germany (S.P.); Pharmaceutical Radiochemistry, Technische Universität München, Garching bei München, Germany (H.-J.W.); and Scintomics GmbH, Fürstfeldbruck, Germany (S.K.).

\*These authors contributed equally to this work.

The online-only Data Supplement is available with this article at <http://hyper.ahajournals.org/lookup/suppl/doi:10.1161/HYPERTENSIONAHA.117.09975/-/DC1>.

Correspondence to Stefanie Hahner, Department of Medicine I, Endocrinology and Diabetes Unit, University of Wuerzburg, Oberduerrbacher Str 6, D-97080 Wuerzburg, Germany. E-mail [hahner\\_s@ukw.de](mailto:hahner_s@ukw.de)

© 2017 American Heart Association, Inc.

*Hypertension* is available at <http://hyper.ahajournals.org>

DOI: 10.1161/HYPERTENSIONAHA.117.09975

the standard procedure in these cases, despite its expense and availability only in major centers.<sup>6,11,12</sup> Moreover, AVS is an invasive technique that is not well standardized between centers and heavily depends on the expertise of the interventional radiologist.<sup>13,14</sup> AVS furthermore requires the use of contrast agents in a patient population that often experiences impaired renal function.<sup>15</sup> To date, proposed clinical prediction scores cannot replace AVS.<sup>16–20</sup> An interesting novel approach consists of the measurement of a selected steroid profile by mass spectrometry.<sup>21,22</sup> Nevertheless, additional diagnostic steps will be needed to localize potential APA.

In this context, functional imaging techniques are of great interest. As a potential target, CYP11B2 (aldosterone synthase) has been investigated, and a selective CYP11B2 inhibitor has recently shown promising results as radiotracer for positron emission tomographic (PET) imaging in first pre-clinical studies.<sup>23</sup>

Chemokines belong to a class of cytokines that exert important physiological effects on organ development, cell migration, and tissue ultrastructure by binding to their specific receptors. In recent years, the role of chemokine receptors in malignant behavior of human cancers has emerged as a particular research focus.<sup>24–26</sup> CXCR4 (CXC chemokine receptor type 4) binds its ligand—the CXC chemokine CXCL12 (stromal cell-derived factor-1). Recently, a second CXCL12 receptor—CXCR7 (the nonclassical/atypical CXC chemokine receptor 7)—has been identified.<sup>27,28</sup> To date, limited data are available on the expression of chemokine receptors in the adrenal cortex, and the presence and functional relevance of chemokine receptors in adrenocortical tumors have not yet been evaluated in detail.

We, therefore, investigated the expression of chemokine receptors in the normal adrenal (NA) and in benign adrenocortical tumors. Because we found high expression of CXCR4 particularly in the zona glomerulosa of the adrenal cortex, we were further interested in the potential of the recently developed CXCR4 ligand 68Ga-pentixafor<sup>29–31</sup> (68GaCPCR4.2) for molecular imaging of aldosterone-producing tissue.

## Materials and Methods

### Availability of Data, Analytical Methods, and Study Materials

The data that support the findings of this study are available from the corresponding author on reasonable request.

### Immunohistochemical Analysis and Quantitative Polymerase Chain Reaction

Immunohistochemistry was performed in formalin-fixed and paraffin-embedded specimens of 2 NAs and 220 patients with known adrenocortical adenomas (117 APAs, 49 NFAs, and 54 cortisol-producing adenomas [CPAs]). The adjacent adrenal cortex was evaluated in 191 of 220 tumor samples. Tissue specimens and corresponding clinical data were derived from 5 tertiary referral centers from the University Hospitals of Berlin, Essen, Munich, Turin, and Wuerzburg. Patients with unilateral APA had been diagnosed according to the 2008 Endocrine Society Practice Guidelines.<sup>32</sup> Collection of patient data and samples was approved by the ethical committees of the respective institutions (Wuerzburg 88/11, Essen 01-187-1787-Z, Charité Berlin EA1/169/08,<sup>33</sup> Munich 379/10, Turin CEI/349). All patients had provided written informed consent.

Chemokine receptor mRNA expression levels were investigated by quantitative real-time polymerase chain reaction. RNA was isolated from fresh frozen tissue of 12 APAs, 11 CPAs, and 3 NFAs using the RNeasy Lipid Tissue Minikit (Qiagen, Alameda, CA) and reversely transcribed using the QuantiTect Reverse Transcription Kit (Qiagen).

For details, please see the [online-only Data Supplement](#).

### Imaging With 68Ga-Pentixafor

Synthesis of 68Ga-pentixafor was performed in Munich and Wuerzburg in a fully automated, good manufacturing practice-compliant procedure using a GRP module (Scintomics GmbH, Fürstenfeldbruck, Germany) equipped with disposable single-use cassette kits (ABX, Radeberg, Germany), using the method and standardized labeling sequence described previously.<sup>30,31,34</sup> Before injection, the quality of 68Ga-pentixafor was assessed according to the standards described in the European Pharmacopoeia for 68Ga-Edotreotide (European Pharmacopoeia, monograph 01/2013:2482, available at [www.edqm.eu](http://www.edqm.eu)). The radiochemical purity of the ready-to-inject formulation as confirmed by radio-high-performance liquid chromatography and radio-thin-layer chromatography was >99%.

In autoradiographic experiments, binding of 68Ga-pentixafor to cryosections from 4 APAs, 4 NFAs, 2 adrenocortical carcinomas, and 3 NAs was analyzed. One slide was treated with 2 MBq 68Ga-pentixafor, and another slide was incubated with 2 MBq 68Ga-pentixafor plus 10  $\mu$ mol/L of nonradioactive compound to monitor specific binding.

To evaluate the suitability of 68Ga-pentixafor for in vivo imaging of APA, 9 patients with APA were investigated: 3 at the University Hospital Wuerzburg (all by PET/computed tomography [CT]) and 6 at the Technical University of Munich (1 patient by PET/CT and 5 patients by PET/magnetic resonance imaging). Reference values for 68Ga-pentixafor uptake in NA glands were established by retrospective analysis of 68Ga-pentixafor-PET imaging results from patients with multiple myeloma (n=20),<sup>29</sup> pleural mesothelioma (n=6), and gastrointestinal tumors (n=18) that had been investigated for individual assessment of eligibility for endoradiotherapy with 177Lu-Pentixafor. In these patients, no adrenal tumor lesion was documented on conventional CT. CT and magnetic resonance imaging scans were scored by a board-certified radiologist, and all PET scans were scored by a board-certified nuclear medicine physician. For details, please see the [online-only Data Supplement](#).

### Statistical Analysis

All statistical tests were performed using either SPSS23 or Graphpad PRISM6. *P* values <0.05 were considered statistically significant. Quantitative values were expressed as mean $\pm$ SEM or median and range as appropriate. Comparisons of related metric measurements were performed using Wilcoxon signed-rank test, and the Mann-Whitney *U* test was used to compare quantitative data between 2 independent samples. In addition, the  $\chi^2$  test was performed for comparison of APA, CPA, and NFA grouped for high or low expression of CXCR4. Correlation between CYP11B2 and CXCR4 staining scores was examined by calculation of Pearson correlation coefficient. Receiver operating characteristic analysis was performed for maximum standardized uptake values (SUV<sub>max</sub> values) of controls and APA with Graphpad PRISM6.

## Results

### Immunohistochemical Analysis of CXCR4, CYP11B1, CYP11B2, and CXCL12

In NA, CXCR4 staining was particularly strong in the subcapsular region. CYP11B2-positive areas exhibited particularly strong CXCR4 expression (Figure 1A). However, the CXCR4-positive area was broader compared with the area of CYP11B2-positive cells. CXCL12 showed a complementary distribution pattern with low expression in the subcapsular area of the adrenal cortex but strong staining in the inner adrenocortical zones (Figure 1A). As for NA, a similar staining



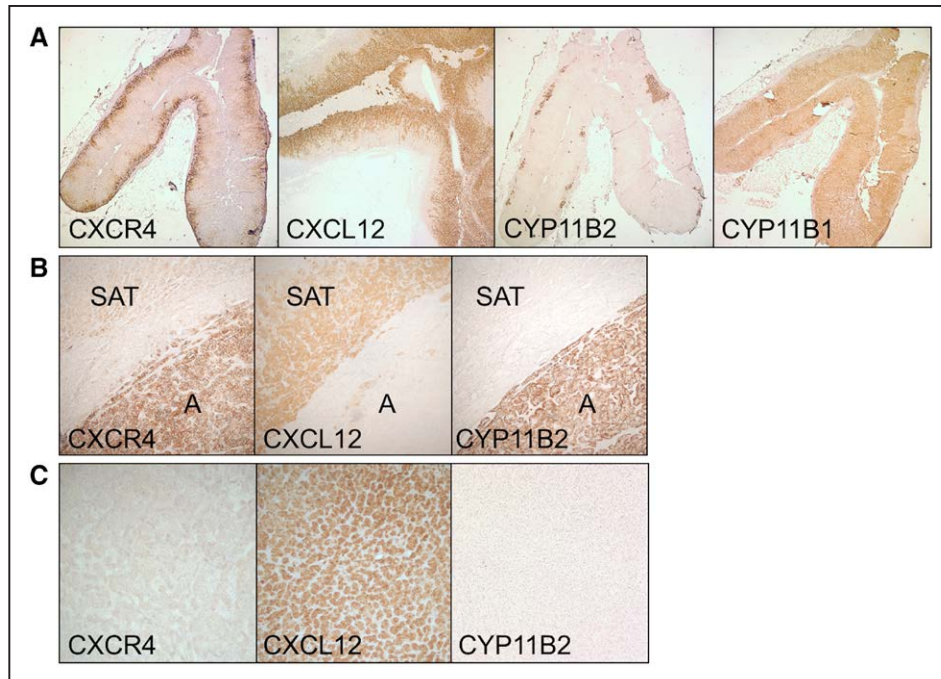


**Figure 1.** CXCR4 (CXC chemokine receptor type 4) staining is particularly high in aldosterone-producing tissue, whereas CXCL12 (stromal cell-derived factor-1) shows a complementary expression pattern. **A**, Immunohistochemical staining of CXCR4, CXCL12, CYP11B2 (aldosterone synthase), and CYP11B1 in the normal adrenal. Magnification  $\times 25$ . Strong CXCR4 staining was detected in the outer part of the normal adrenal cortex covering a broader and more continuous area compared with CYP11B2, which was predominantly found in subcapsular aldosterone-producing cell clusters. CXCL12 showed a complementary staining pattern to CXCR4 with missing expression in the outer cortical part but strong staining in the inner adrenocortical zones. **B**, Representative images for aldosterone-producing adenoma (APA). Strong CXCR4 staining was observed in the APA, which correlated with CYP11B2 staining, whereas CXCL12 staining was observed only in the surrounding adrenocortical tissue (SAT). Magnification  $\times 10$ . **C**, Representative images for nonfunctioning adenoma (NFA). Immunohistochemical staining for CXCR4 and CYP11B2 was negative; in contrast, strong CXCL12 staining was observed in the adenoma (A). Magnification  $\times 10$ .

pattern was found for CXCR4 and CXCL12 in APA ( $n=5$ ), CPA ( $n=5$ ), and NFA ( $n=5$ ; Figure 1B and 1C). CXCR7 was expressed equally in all adrenocortical zones (data not shown).

In adrenocortical adenomas, high CXCR4 membrane staining was found in 71% of APAs (Figure 1B; Figure S2 in the [online-only Data Supplement](#)), 26% of CPAs and 4% of NFAs. Eight NFAs were completely CXCR4 negative (Table 1).

Comparison of membrane staining intensity revealed highly significant differences between NFA and APA ( $P<0.001$ ). Likewise, a significant positive correlation was observed between CXCR4 membrane staining and CYP11B2 staining intensity in APA ( $r=0.42$ ;  $P<0.01$ ). CYP11B1 was coexpressed in 81% of APAs, 100% of CPAs and 98% of NFAs (Table 2).

CXCR4 immunostaining was observed in all adjacent adrenal cortices independent of the underlying adrenal tumor (Table 1).

No differences were observed on clinical parameters or mutational status among patients with APA when grouping them according to the CXCR4 staining intensity of their respective tumor (Table 2).

### Quantitative Analysis of Chemokine Receptor Expression

Quantitative real-time polymerase chain reaction revealed high mRNA levels for CXCR4 and CXCR7 in all adrenocortical

tumor tissues. However, CXCR4 and CXCR7 expression showed considerable variation and did not differ significantly between adenoma types at mRNA level. Furthermore, other chemokine receptors were found to be expressed at lower

**Table 1. CXCR4 Protein Expression in Samples From Standard Full Slides in 117 APAs, 54 CPAs, and 49 NFAs**

| CXCR4            |          | Low Membrane Staining, n (%) | High Membrane Staining, n (%) |
|------------------|----------|------------------------------|-------------------------------|
| <i>h</i> score   | <i>n</i> | $\leq 1$                     | $> 1$                         |
| APA              | 117      | 34 (29%)                     | 83 (71%)                      |
| CPA              | 54       | 40 (74%)                     | 14 (26%)                      |
| NFA              | 49       | 47 (96%)                     | 2 (4%)                        |
| Adjacent adrenal |          |                              |                               |
| APA              | 108      | 66 (61%)                     | 42 (39%)                      |
| CPA              | 47       | 31 (66%)                     | 16 (34%)                      |
| NFA              | 36       | 26 (72%)                     | 10 (28%)                      |

Semiquantitative *h* score was calculated by multiplying the staining intensity grading score with the proportion score (0.1=1%–9%, 0.5=10%–49%, 1=50% or more cells with CXCR4 staining, respectively). Significant differences were observed for comparison of APA with NFA and also for comparison of APA with CPA,  $P<0.001$ , respectively. CPA versus NFA,  $P=0.002$ . No significant differences between tumor entities were observed for CXCR4 membrane staining intensity in adjacent adrenal cortex. APA indicates aldosterone-producing adenoma; CPA, cortisol-producing adenoma; CXCR4, CXC chemokine receptor type 4; and NFA, nonfunctioning adenoma.

**Table 2. Clinical Parameters of Patients With APA Included in the Immunohistochemical Analysis**

| Patient Data   | CXCR4             | CXCR4             | P Value |
|--|-------------------|-------------------|---------|
|  | <i>h</i> score ≤1 | <i>h</i> score >1 |         |
|  | n=34              | n=83              |         |
| Age at diagnosis, y (median; range)                                  | 49 (26–67)        | 49 (18–75)        | 0.9     |
| Sex (M/F), %   | 44/56             | 39/61             | 0.6     |
| SBP, mm Hg   | 170±22            | 160±26            | 0.1     |
| DBP, mm Hg   | 100±11.5          | 100±15            | 0.2     |
| Serum potassium, mmol/L  | 3.0±0.6           | 3.0±0.7           | 0.9     |
| Plasma aldosterone, ng/L   | n=23              | n=48              | 0.5     |
|  | 520 (208–1950)    | 500 (57–1148)     |         |
| Mutation status of APA, n  | 25                | 58                | 0.1     |
| WT   | 15                | 23                |         |
| KCNJ5  | 7                 | 28                |         |
| ATPAS  | 1                 | 5                 |         |
| CACNA1D  | 2                 | 2                 |         |
| Additional CYP11B1 expression detected by IHC (percentage of tumors) | 73                | 84                | 0.2     |

Group comparison according to CXCR4 membrane staining of the respective APA. No statistically significant differences were found between groups. APA indicates aldosterone-producing adenoma; ATPAS, ATPase (Na/K-ATPase); CACNA1D, calcium voltage-gated channel subunit alpha1 D; CXCR4, CXC chemokine receptor type 4; DBP, diastolic blood pressure; F, female; IHC, immunohistochemistry; KCNJ5, G protein-activated inward rectifier potassium channel 4; M, male; SBP, systolic blood pressure; and WT, wild type.

levels, especially CCR11, CCR7, and CCR3 (C-C chemokine receptor types 11, 7 and 3) in NA and CXCR2 (CXC chemokine receptor type 2), CCR2 (C-C chemokine receptor type 2), and CCR11 in APA, CPA, and NFA (Figure 2).

### Autoradiographic Experiments With 68Ga-Pentixafor

Autoradiographic visualization of 68Ga-pentixafor revealed strong specific binding to APA and adrenocortical carcinoma tissues and the outer cortical zones of the NA (Figure 3A). No binding was observed to NFA.

### 68Ga-Pentixafor PET Imaging In Vivo

Further information on patients with PA, results of imaging, AVS, and clinical outcome is given in Table 3. 68Ga-pentixafor uptake in the area of the adrenal nodule of patients with PA was observed with median  $SUV_{max}=8.6$  (4.7–18.3), in the contralateral adrenal values were significantly lower:  $SUV_{max}=4.0$  (2.3–6.5;  $P<0.001$ ). Only 1 patient with a 6-mm tumor showed lower 68Ga-pentixafor uptake at the side of surgery. In the control group,  $SUV_{max}$  values ranged from 1.0 to 5.8 (mean  $SUV_{max}$ : left adrenal gland, 3.4; right adrenal gland, 3.0; Figure 3D). Histopathology confirmed the tumors to be adrenocortical adenomas. CXCR4 immunoreactivity was investigated in 4 patients being strongly positive for CXCR4 (*h* score, 2 in 3 cases and *h* score, 3 in 1 case). All tumors also showed positive CYP11B2 staining.

Additionally, ratios were calculated for  $SUV_{max}$  values by dividing the higher SUV through the lower level of the respective contralateral side in controls and by dividing the  $SUV_{max}$  value of the side of APA through the contralateral side in patients with PA. Ratios from patients with APA significantly differed from ratios of controls (APA: mean,  $2.8\pm0.5$ ; control: mean,  $1.5\pm0.08$ ;  $P<0.001$ ). In receiver operating characteristic analysis, a cutoff value for  $SUV_{max}$  of 4.9 revealed a sensitivity of 88.9% (95% confidence interval, 51.8–99.7) and a specificity of 87.2% (95% confidence interval, 78.3–93.4) for diagnosing APA. Setting specificity to 100% a cutoff value of 7.3 was calculated (sensitivity, 77.8%), whereas a sensitivity of 100% was reached at a cutoff value of 4.7 (specificity, 83.7%). Area under the curve was 0.964 (95% confidence interval, 0.92–1.01; Figure 3E).

### Discussion

The key in vitro finding of our investigation is the high expression of the chemokine receptors CXCR4 and CXCR7 in aldosterone-producing tissue. In contrast, expression of CXCR4 was negative or only weak in almost all nonfunctioning adrenocortical adenomas. Based on this differential expression pattern, we investigated the available PET tracer 68Ga-pentixafor, which selectively binds to human CXCR4,<sup>29,35</sup> thus representing a potentially suitable imaging biomarker for noninvasive differential diagnosis in PA.

Quantitative real-time polymerase chain reaction revealed the expression of several chemokine receptors in both NA and adrenocortical adenomas. The most highly expressed receptors were CXCR7 and CXCR4: the high expression levels found in NAs suggest an important role in adrenal physiology. Interestingly, CXCR4 protein expression in the adrenal cortex was particularly high in the outer part of the adrenal cortex. In contrast, immunohistochemical staining of its ligand CXCL12 was highest in the inner adrenocortical zones. Because migration of CXCR4-expressing cells along a CXCL12 gradient has been demonstrated for different cells,<sup>26,36</sup> it is possible to speculate that the expression pattern of CXCR4 and CXCL12 is involved in the proposed centripetal migration and transdifferentiation of adrenocortical cells. In this model, it is hypothesized that undifferentiated progenitor cells in the subcapsular region give rise to differentiated mineralocorticoid-producing zona glomerulosa cells, which migrate centripetally and undergo lineage conversion into glucocorticoid-producing zona fasciculata and reticularis cells.<sup>37,38</sup> In this context, the CXCL12 gradient might play a major role for the migration direction of adrenocortical cells. An alternative hypothesis is that the observed expression pattern is relevant for the ultrastructural organization of the adrenal cortex and local cell–cell interaction as has been shown for other tissues.<sup>39,40</sup> CXCR7 also binds CXCL12. It has been shown to exert a scavenger function and modulate CXCL12–CXCR4 signaling.<sup>41</sup> However, the precise physiological role of the CXCL12/CXCR4/CXCR7 system in the NA remains to be elucidated.

Corresponding to the high expression of CXCR4 in the outer adrenal cortex, high expression levels were also found in APA, whereas expression in NFA was almost negligible. CXCR4 expression and CYP11B2 expression levels

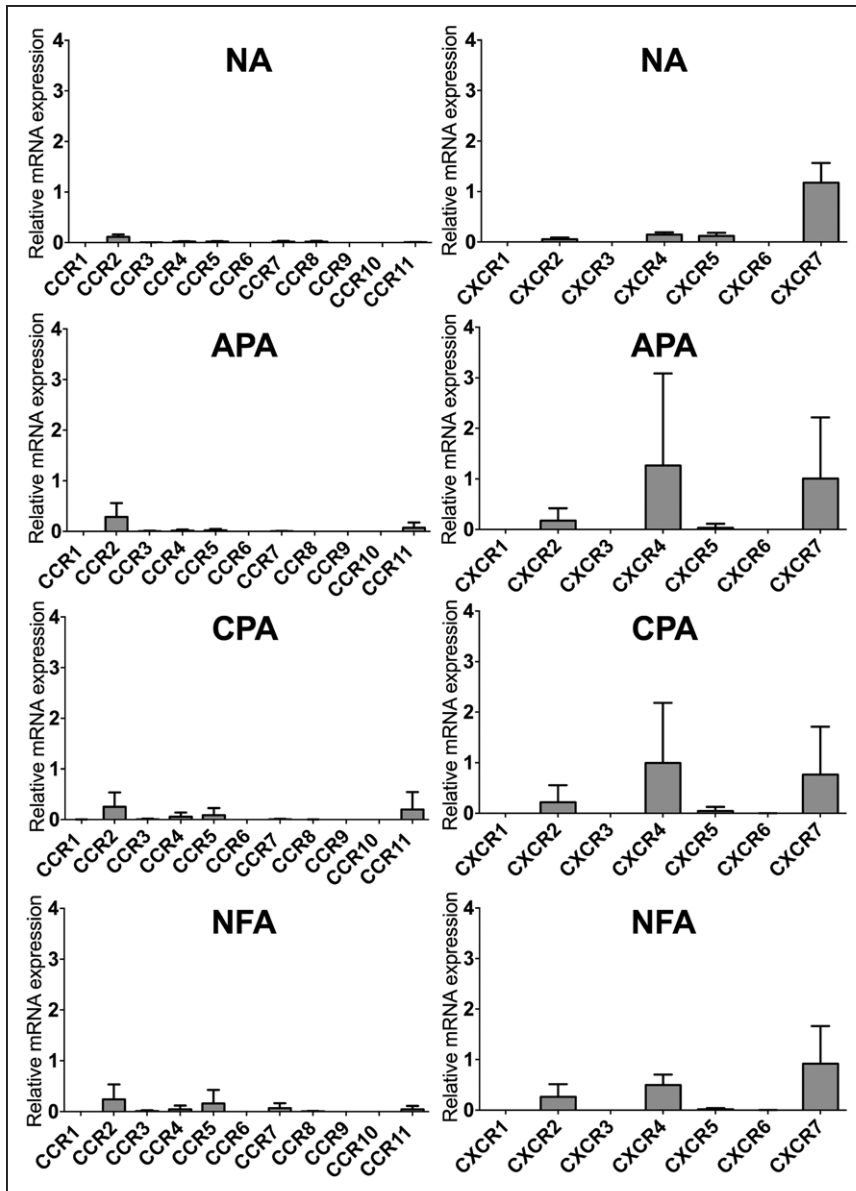


**Figure 2.** Chemokine receptor mRNA expression in adrenocortical adenomas. Relative chemokine receptor mRNA expression of CC chemokine receptors (**left**) and CXC chemokine receptors (**right**) in normal adrenal (NA, n=4), aldosterone-producing adenoma (APA, n=12), cortisol-producing adenoma (CPA, n=11), and nonfunctioning adenoma (NFA, n=3).

correlated significantly, further emphasizing the particularly high expression of CXCR4 in aldosterone-producing tissue, which was independent of sex, clinical parameters, or mutational status. On the background of these findings,  $^{68}\text{Ga}$ -pentixafor PET imaging might be a useful tool for non-invasive characterization of adrenal lesions in PA. The results from the autoradiographic studies fit well with the findings from our immunohistochemical analyses. Strong binding of  $^{68}\text{Ga}$ -pentixafor could be documented for APA and parts of the NA cortex in contrast to NFA that did not show relevant tracer binding.

$^{11}\text{C}$ -metomidate PET imaging has recently been used in patients with primary PA and was able to identify aldosterone-producing tissue in these patients with high imaging quality. Metomidate binds to both enzymes CYP11B1 and CYP11B2 with high avidity.<sup>42</sup> Our observation of expression of both CYP11B1 and CYP11B2 in most APAs matches with the observed high  $^{11}\text{C}$ -metomidate uptake in the aldosterone-producing tissue.<sup>43,44</sup> However, 98% of the NFAs in our series

also exhibited CYP11B1 staining, and both  $^{11}\text{C}$ -metomidate uptake and  $^{123}\text{I}$ -iodometomidate uptake in NFA have been demonstrated in clinical studies.<sup>45,46</sup> CYP11B1 downregulation may be achieved in normal surrounding adrenocortical tissue by dexamethasone pretreatment. However, it is unclear whether this also holds true for adrenocortical adenoma cells because ACTH (adrenocorticotrophic hormone) receptor expression is low in NFAs.<sup>47</sup> Nevertheless, the data obtained by the  $^{11}\text{C}$ -metomidate studies represent an important proof of principle demonstrating that the PET imaging technique per se may be of value in PA.<sup>44</sup>

Targeting CXCR4 in PA may be a promising alternative approach. This is highlighted by our 9 patients with APA who were investigated by  $^{68}\text{Ga}$ -pentixafor PET/CT. All patients showed focal  $^{68}\text{Ga}$ -pentixafor uptake in the adrenal nodule with  $\text{SUV}_{\text{max}}$  values ranging between 4.7 and 18.3 (mean, 10.7), whereas the mean  $\text{SUV}_{\text{max}}$  value measured in non-PA patients was 3.3. Uptake values in APA significantly differed both from values obtained in controls and in the contralateral



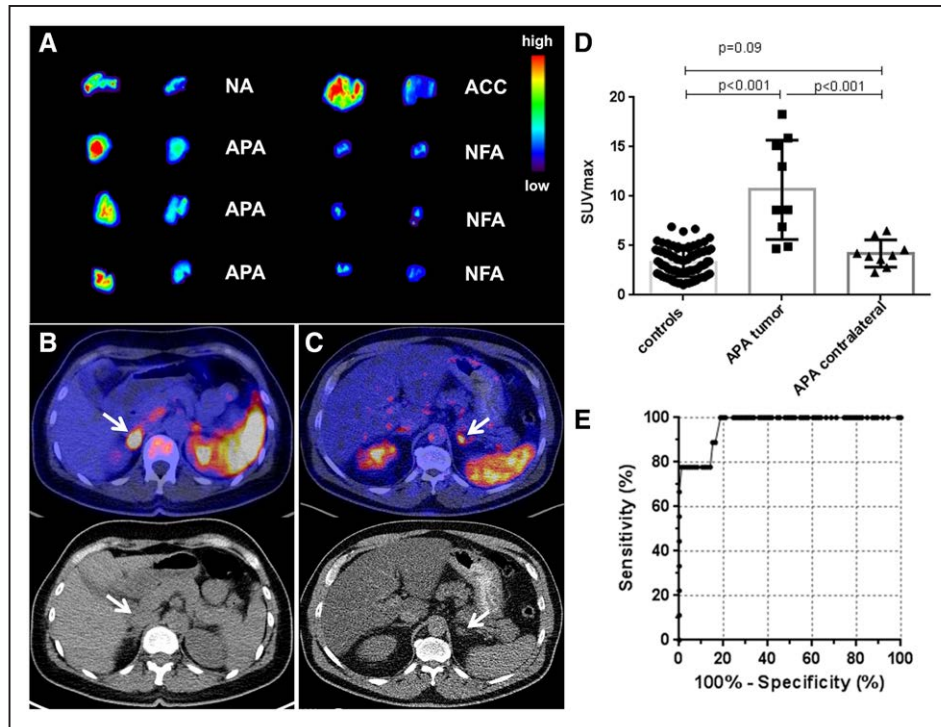


**Figure 3.** The CXCR4 (CXC chemokine receptor type 4) ligand 68Ga-pentixafor specifically accumulates in aldosterone-producing tissue. Ex vivo experiments and clinical positron emission tomographic (PET) imaging. **A**, Ex vivo autoradiographic visualization of 68Ga-pentixafor binding to cryosections of the normal adrenal gland (NA), aldosterone-producing adenoma (APA), adrenocortical carcinoma (ACC), and nonfunctioning adenoma (NFA). Red colors indicate highest binding of radio ligand, blue/dark blue colors indicate no binding or full competitive inhibition. **A**, 2MBq 68Ga-pentixafor; **B**, 2MBq 68Ga-pentixafor plus 10  $\mu$ M of the nonradioactive ligand. Strong ligand binding that could be blocked by coinubation with the unlabeled tracer compound could be documented in NA, APA, and ACC. **B** and **C**, Representative images of 68Ga-pentixafor PET/computed tomographic (CT) imaging in 2 patients with APA: 68Ga-pentixafor imaging in a 47-year-old female patient with primary aldosteronism after injection of 152 MBq 68Ga-pentixafor (**B**). 68Ga-pentixafor-PET/CT of a 66-year-old male patient with primary aldosteronism after injection of 126 MBq 68Ga-pentixafor (**C**). White arrows indicate the tumor lesion. **D**, Maximum standardized uptake values (SUV<sub>max</sub>) for 68Ga-pentixafor uptake in the adrenal of control subjects compared with patients with APA both at the tumor (APA tumor) and the contralateral (APA contralateral) side. Adrenal SUV<sub>max</sub> values from controls are pooled data derived from both sides. **E**, Receiver operating characteristic analysis of SUV<sub>max</sub> values. Data were obtained from controls (n=44; 86 values were obtained from measurement of the left and right adrenal; in 2 patients, only the left adrenal was available) and 9 APAs. A cutoff value for SUV<sub>max</sub> of 4.8 revealed a sensitivity of 89% (95% confidence interval [CI], 51.8–99.7) and a specificity of 85% (95% CI, 75.5–91.7). Setting specificity to 100% a cutoff value of 7.8 was calculated (sensitivity, 67%), whereas a sensitivity of 100% was reached at a cutoff value of 4.7 (specificity, 81%). Area under the curve, 0.964 (95% CI, 0.92–1.01).

adrenals. In 1 patient, APA measured only 6 mm and was not detected by 68Ga-pentixafor indicating the detection limit for small lesions because of reduced spatial resolution. In 2 patients, 68Ga-pentixafor identified the tumor side, which was unable to be localized by AVS.

As a future approach, the combination of steroid profiling by mass spectrometry as a first differential diagnostic step with subsequent functional imaging using 68Ga-pentixafor PET/CT or 68Ga-pentixafor PET/magnetic resonance imaging could enable noninvasive diagnosis in most patients with PA. As furthermore 96% of NFA exhibited either low or no staining for CXCR4, no tracer uptake would be expected in these tumors. Because immunohistochemistry revealed low CXCR4 staining in 29% of APAs, only this subgroup would remain for further investigation by AVS. A small group of patients with NFA is expected to be false-positive in 68Ga-pentixafor PET imaging because 2 of these adenomas (4%) in our series showed high CXCR4 expression. On the contrary, we recently found high CXCR4 expression in adrenocortical carcinoma.<sup>48</sup> Therefore, a high CXCR4 uptake in PET

imaging generally might be associated with a lower threshold for the decision for surgery. However, this would need to be corroborated by further studies. In both NFA patients with strong CXCR4 staining in our cohort, tumor growth was documented leading to the decision for adrenalectomy.

There are several limitations on the clinical aspects of our article: within this translational project, we did not perform a standardized clinical trial investigating healthy individuals, and the data used as controls were obtained from patient cohorts with malignant disease that had already undergone 68Ga-pentixafor PET imaging for other clinical reasons. It is to date unclear whether concurrent chemotherapy might influence CXCR4 expression in vivo. Many malignant tumors exhibit high CXCR4 expression, and although no adrenal metastases were detected by conventional imaging, CXCR4-positive micrometastases could not be excluded. Subgroup analysis of the 3 groups of control patients who received different treatments did, however, not reveal any group differences. Uptake values in the contralateral adrenals of patients with PA were not significantly higher compared with the controls without PA.



**Table 3. Clinical Parameters of 9 Patients With Aldosterone-Producing Adenoma Investigated by 68Ga-Pentixafor**

| Sex | Age, y | TU Side in CI | TU Size, mm | AVS, Result                            | SUV <sub>max</sub> <sup>1</sup> Right | SUV <sub>max</sub> <sup>1</sup> Left | Surgery    | Outcome |
|-----|--------|---------------|-------------|--|---------------------------------------|--------------------------------------|------------|---------|
| F   | 47     | R             | 23          | Unsuccessful sampling R, suppression L | 13.0                                  | 3.6                                  | R          | CBR     |
| F   | 57     | R             | 17          | Lateralization R, no suppression L     | 15.1                                  | 2.8                                  | R          | CBR     |
| F   | 55     | R             | 37          | No lateralization                      | 8.6                                   | 4.0                                  | R          | CBR     |
| M   | 50     | R             | 6           | Lateralization R                       | 4.9                                   | 6.1                                  | R          | CBR     |
| F   | 47     | R             | 14          | No AVS                                 | 18.3                                  | 4.2                                  | R          | CBR     |
| M   | 63     | L             | 18          | Lateralization L                       | 2.3                                   | 4.7                                  | L          | CBR     |
| M   | 57     | L             | 28          | No lateralization                      | 3.9                                   | 15.9                                 | L          | CBR     |
| M   | 44     | ...           | No TU       | Lateralization R                       | 6.9                                   | 6.5                                  | No surgery | ...     |
| M   | 65     | L             | 12          | Lateralization L                       | 4.6                                   | 8.6                                  | No surgery | ...     |

AVS indicates adrenal vein sampling; CBR, clinical improvement and biochemical remission; CI, conventional imaging; F, female; L, left; M, male; R, right; SUV<sub>max</sub>, maximum standardized uptake value; and TU, tumor.

In our patient series, most tumor lesions were >1 cm. Many APAs are <1 cm, which generally limits the sensitivity of PET imaging because of the reduced spatial resolution of this imaging approach.<sup>49</sup> Thus, 68Ga-pentixafor PET imaging may not fully replace but at least significantly reduce the number of AVS to a more selected patient subgroup.

### Perspectives

Taken together, we have demonstrated that CXCR4 is highly abundant in the zona glomerulosa and in APAs suggesting a significant role in adrenocortical physiology and further representing a potential target for molecular imaging of aldosterone-producing tissue. Considering the need for universal diagnostic alternatives to AVS in PA, 68Ga-pentixafor PET represents a novel and promising tool for differential diagnosis that warrants further evaluation in a prospective clinical trial.

### Acknowledgments

We thank all colleagues of Nuclear Medicine and the Endocrine Unit, Department of Medicine I, University of Wuerzburg, for excellent cooperation. B. Heinze, C.T. Fuss, and S. Hahner designed and performed in vitro experiments, collected and analyzed preclinical and clinical data, and wrote the article. K. Lang contributed to preclinical experiments; A. Schirbel performed radiosyntheses; P. Mulatero, F. Beuschlein, M. Reincke, T.A. Williams, M. Quinkler, N. Rayes, V. Wild, A.-C. Reis, S. Petersenn, T. Deutschbein, S. Monticone, Y. Rhayem, and M. Fassnacht provided biomaterials and clinical patient data; C.E. Gomez-Sanchez provided selective antibodies detecting human CYP11B1 and CYP11B2; M. Mustafa, C. Bluemel, K. Herrmann, and A.K. Buck performed patient imaging and analysis of imaging data; H.-J. Wester and S. Kropf provided the precursor for 68Ga-pentixafor. The article was edited and approved by all authors.

### Sources of Funding

This work was supported by the Deutsche Forschungsgemeinschaft (AL 203/I-1 to A.K. Buck, A. Schirbel, and S. Hahner; SFB-TR-B13 to S. Hahner and M. Reincke; and RE 752/20-1 to M. Reincke) and the Else Kröner-Fresenius-Stiftung (No. 2013\_A49 to S. Hahner and

A. Schirbel, and 2015\_A171 and 2013\_A182 to M. Reincke). M. Reincke is supported by the European Research Council under the European Union Horizon 2020 program (No. 694913).

### Disclosures

H.-J. Wester is the Chief Executive Officer (CEO) and shareholder of Scintomics. S. Kropf is the CEO of Scintomics. The other authors report no conflicts.

### References

1. Stowasser M. Primary aldosteronism in 2011: towards a better understanding of causation and consequences. *Nat Rev Endocrinol*. 2011;8:70–72. doi: 10.1038/nrendo.2011.223.
2. Born-Frontsberg E, Reincke M, Rump LC, Hahner S, Diederich S, Lorenz R, Allolio B, Seufert J, Schirpenbach C, Beuschlein F, Bidlingmaier M, Endres S, Quinkler M; Participants of the German Conn's Registry. Cardiovascular and cerebrovascular comorbidities of hypokalemic and normokalemic primary aldosteronism: results of the German Conn's Registry. *J Clin Endocrinol Metab*. 2009;94:1125–1130. doi: 10.1210/jc.2008-2116.
3. Hanslik G, Wallaschofski H, Dietz A, Riester A, Reincke M, Allolio B, Lang K, Quack I, Rump LC, Willenberg HS, Beuschlein F, Quinkler M, Hannemann A; participants of the German Conn's Registry. Increased prevalence of diabetes mellitus and the metabolic syndrome in patients with primary aldosteronism of the German Conn's Registry. *Eur J Endocrinol*. 2015;173:665–675. doi: 10.1530/EJE-15-0450.
4. Mulatero P, Stowasser M, Loh KC, Fardella CE, Gordon RD, Mosso L, Gomez-Sanchez CE, Veglio F, Young WF Jr. Increased diagnosis of primary aldosteronism, including surgically correctable forms, in centers from five continents. *J Clin Endocrinol Metab*. 2004;89:1045–1050. doi: 10.1210/jc.2003-031337.
5. Rossi GP, Bernini G, Caliumi C, et al; PAPY Study Investigators. A prospective study of the prevalence of primary aldosteronism in 1,125 hypertensive patients. *J Am Coll Cardiol*. 2006;48:2293–2300. doi: 10.1016/j.jacc.2006.07.059.
6. Funder JW, Carey RM, Mantero F, Murad MH, Reincke M, Shibata H, Stowasser M, Young WF Jr. The management of primary aldosteronism: case detection, diagnosis, and treatment: an Endocrine Society Clinical Practice Guideline. *J Clin Endocrinol Metab*. 2016;101:1889–1916. doi: 10.1210/jc.2015-4061.
7. Fassnacht M, Arlt W, Bancos I, Dralle H, Newell-Price J, Sahdev A, Tabarin A, Terzolo M, Tsagarakis S, Dekkers OM. Management of adrenal incidentalomas: European Society of Endocrinology Clinical Practice Guideline in collaboration with the European Network for the Study of Adrenal Tumors. *Eur J Endocrinol*. 2016;175:G1–G34. doi: 10.1530/EJE-16-0467.

8. Young WF, Stanson AW, Thompson GB, Grant CS, Farley DR, van Heerden JA. Role for adrenal venous sampling in primary aldosteronism. *Surgery*. 2004;136:1227–1235. doi: 10.1016/j.surg.2004.06.051.
9. Nwariaku FE, Miller BS, Auchus R, Holt S, Watumull L, Dolmatch B, Nesbitt S, Vongpatanasin W, Victor R, Wians F, Livingston E, Snyder WH III. Primary hyperaldosteronism: effect of adrenal vein sampling on surgical outcome. *Arch Surg*. 2006;141:497–502; discussion 502. doi: 10.1001/archsurg.141.5.497.
10. Kempers MJ, Lenders JW, van Outheusden L, van der Wilt GJ, Schultze Kool LJ, Hermus AR, Deinum J. Systematic review: diagnostic procedures to differentiate unilateral from bilateral adrenal abnormality in primary aldosteronism. *Ann Intern Med*. 2009;151:329–337.
11. Stewart PM, Allolio B. Adrenal vein sampling for primary aldosteronism: time for a reality check. *Clin Endocrinol (Oxf)*. 2010;72:146–148. doi: 10.1111/j.1365-2265.2009.03714.x.
12. Dekkers T, Prejbisz A, Kool LJS, et al; SPARTACUS Investigators. Adrenal vein sampling versus CT scan to determine treatment in primary aldosteronism: an outcome-based randomised diagnostic trial. *Lancet Diabetes Endocrinol*. 2016;4:739–746. doi: 10.1016/S2213-8587(16)30100-0.
13. Vonend O, Ockenfels N, Gao X, et al; German Conn's Registry. Adrenal venous sampling: evaluation of the German Conn's Registry. *Hypertension*. 2011;57:990–995. doi: 10.1161/HYPERTENSIONAHA.110.168484.
14. Rossi GP, Barisa M, Allolio B, et al. The Adrenal Vein Sampling International Study (AVIS) for identifying the major subtypes of primary aldosteronism. *J Clin Endocrinol Metab*. 2012;97:1606–1614. doi: 10.1210/jc.2011-2830.
15. Reincke M, Rump LC, Quinkler M, Hahner S, Diederich S, Lorenz R, Seufert J, Schirpenbach C, Beuschlein F, Bidlingmaier M, Meisinger C, Holle R, Endres S; Participants of German Conn's Registry. Risk factors associated with a low glomerular filtration rate in primary aldosteronism. *J Clin Endocrinol Metab*. 2009;94:869–875. doi: 10.1210/jc.2008-1851.
16. Riester A, Fischer E, Degenhart C, Reiser MF, Bidlingmaier M, Beuschlein F, Reincke M, Quinkler M. Age below 40 or a recently proposed clinical prediction score cannot bypass adrenal venous sampling in primary aldosteronism. *J Clin Endocrinol Metab*. 2014;99:E1035–E1039. doi: 10.1210/jc.2013-3789.
17. Mulatero P, Bertello C, Rossato D, Mengozzi G, Milan A, Garrone C, Giraudo G, Passarino G, Garaballo D, Verhovez A, Rabbia F, Veglio F. Roles of clinical criteria, computed tomography scan, and adrenal vein sampling in differential diagnosis of primary aldosteronism subtypes. *J Clin Endocrinol Metab*. 2008;93:1366–1371. doi: 10.1210/jc.2007-2055.
18. Venos ES, So B, Dias VC, Harvey A, Pasieka JL, Kline GA. A clinical prediction score for diagnosing unilateral primary aldosteronism may not be generalizable. *BMC Endocr Disord*. 2014;14:94. doi: 10.1186/1472-6823-14-94.
19. Sze WC, Soh LM, Lau JH, et al. Diagnosing unilateral primary aldosteronism - comparison of a clinical prediction score, computed tomography and adrenal venous sampling. *Clin Endocrinol (Oxf)*. 2014;81:25–30. doi: 10.1111/cen.12374.
20. Küpers EM, Amar L, Raynaud A, Plouin PF, Steichen O. A clinical prediction score to diagnose unilateral primary aldosteronism. *J Clin Endocrinol Metab*. 2012;97:3530–3537. doi: 10.1210/jc.2012-1917.
21. Williams TA, Peitzsch M, Dietz AS, Dekkers T, Bidlingmaier M, Riester A, Treitl M, Rhayem Y, Beuschlein F, Lenders JW, Deinum J, Eisenhofer G, Reincke M. Genotype-specific steroid profiles associated with aldosterone-producing adenomas. *Hypertension*. 2016;67:139–145. doi: 10.1161/HYPERTENSIONAHA.115.06186.
22. Eisenhofer G, Dekkers T, Peitzsch M, Dietz AS, Bidlingmaier M, Treitl M, Williams TA, Bornstein SR, Haase M, Rump LC, Willenberg HS, Beuschlein F, Deinum J, Lenders JW, Reincke M. Mass spectrometry-based adrenal and peripheral venous steroid profiling for subtyping primary aldosteronism. *Clin Chem*. 2016;62:514–524. doi: 10.1373/clinchem.2015.251199.
23. Abe T, Naruse M, Young WF Jr, Kobashi N, Doi Y, Izawa A, Akama K, Okumura Y, Ikenaga M, Kimura H, Saji H, Mukai K, Matsumoto H. A novel CYP11B2-specific imaging agent for detection of unilateral subtypes of primary aldosteronism. *J Clin Endocrinol Metab*. 2016;101:1008–1015. doi: 10.1210/jc.2015-3431.
24. Müller A, Homey B, Soto H, Ge N, Catron D, Buchanan ME, McClanahan T, Murphy E, Yuan W, Wagner SN, Barrera JL, Mohar A, Verástegui E, Zlotnik A. Involvement of chemokine receptors in breast cancer metastasis. *Nature*. 2001;410:50–56. doi: 10.1038/35065016.
25. Chatterjee S, Behnam Azad B, Nimmagadda S. The intricate role of CXCR4 in cancer. *Adv Cancer Res*. 2014;124:31–82. doi: 10.1016/B978-0-12-411638-2.00002-1.
26. Wang J, Knaut H. Chemokine signaling in development and disease. *Development*. 2014;141:4199–4205. doi: 10.1242/dev.101071.
27. Balabanian K, Lagane B, Infantino S, Chow KY, Harriague J, Moepps B, Arenzana-Seisdedos F, Thelen M, Bachelier F. The chemokine SDF-1/CXCL12 binds to and signals through the orphan receptor RDC1 in T lymphocytes. *J Biol Chem*. 2005;280:35760–35766. doi: 10.1074/jbc.M508234200.
28. Burns JM, Summers BC, Wang Y, Melikian A, Berahovich R, Miao Z, Penfold ME, Sunshine MJ, Littman DR, Kuo CJ, Wei K, McMaster BE, Wright K, Howard MC, Schall TJ. A novel chemokine receptor for SDF-1 and I-TAC involved in cell survival, cell adhesion, and tumor development. *J Exp Med*. 2006;203:2201–2213. doi: 10.1084/jem.20052144.
29. Philipp-Abbrederis K, Herrmann K, Knop S, et al. *In vivo* molecular imaging of chemokine receptor CXCR4 expression in patients with advanced multiple myeloma. *EMBO Mol Med*. 2015;7:477–487. doi: 10.15252/emmm.201404698.
30. Demmer O, Dijkgraaf I, Schumacher U, Marinelli L, Cosconati S, Gourni E, Wester HJ, Kessler H. Design, synthesis, and functionalization of dimeric peptides targeting chemokine receptor CXCR4. *J Med Chem*. 2011;54:7648–7662. doi: 10.1021/jm2009716.
31. Demmer O, Gourni E, Schumacher U, Kessler H, Wester HJ. PET imaging of CXCR4 receptors in cancer by a new optimized ligand. *ChemMedChem*. 2011;6:1789–1791. doi: 10.1002/cmdc.201100320.
32. Funder JW, Carey RM, Fardella C, Gomez-Sanchez CE, Mantero F, Stowasser M, Young WF Jr, Montori VM; Endocrine Society. Case detection, diagnosis, and treatment of patients with primary aldosteronism: an Endocrine Society Clinical Practice Guideline. *J Clin Endocrinol Metab*. 2008;93:3266–3281. doi: 10.1210/jc.2008-0104.
33. Monticone S, Castellano I, Versace K, Lucatello B, Veglio F, Gomez-Sanchez CE, Williams TA, Mulatero P. Immunohistochemical, genetic and clinical characterization of sporadic aldosterone-producing adenomas. *Mol Cell Endocrinol*. 2015;411:146–154. doi: 10.1016/j.mce.2015.04.022.
34. Martin R, Jüttler S, Müller M, Wester HJ. Cationic eluate pretreatment for automated synthesis of [<sup>68</sup>Ga]CPCRA4.2. *Nucl Med Biol*. 2014;41:84–89. doi: 10.1016/j.nucmedbio.2013.09.002.
35. Herrmann K, Lapa C, Wester HJ, Schottelius M, Schiepers C, Eberlein U, Bluemel K, Keller U, Knop S, Kropf S, Schirbel A, Buck AK, Lassmann M. Biodistribution and radiation dosimetry for the chemokine receptor CXCR4-targeting probe 68Ga-pentixafor. *J Nucl Med*. 2015;56:410–416. doi: 10.2967/jnumed.114.151647.
36. Zlotnik A, Burkhardt AM, Homey B. Homeostatic chemokine receptors and organ-specific metastasis. *Nat Rev Immunol*. 2011;11:597–606. doi: 10.1038/nri3049.
37. Xing Y, Lerario AM, Rainey W, Hammer GD. Development of adrenal cortex zonation. *Endocrinol Metab Clin North Am*. 2015;44:243–274. doi: 10.1016/j.ecl.2015.02.001.
38. Freedman BD, Kempna PB, Carlone DL, Shah M, Guagliardo NA, Barrett PQ, Gomez-Sanchez CE, Majzoub JA, Breault DT. Adrenocortical zonation results from lineage conversion of differentiated zona glomerulosa cells. *Dev Cell*. 2013;26:666–673. doi: 10.1016/j.devcel.2013.07.016.
39. Haeghe S, Einer C, Thiele S, Mueller W, Nietzsche S, Lupp A, Mackay F, Schulz S, Stumm R. CXC chemokine receptor 7 (CXCR7) regulates CXCR4 protein expression and capillary tuft development in mouse kidney. *PLoS One*. 2012;7:e42814. doi: 10.1371/journal.pone.0042814.
40. Hunger C, Ödemis V, Engele J. Expression and function of the SDF-1 chemokine receptors CXCR4 and CXCR7 during mouse limb muscle development and regeneration. *Exp Cell Res*. 2012;318:2178–2190. doi: 10.1016/j.yexcr.2012.06.020.
41. Memi F, Abe P, Cariboni A, MacKay F, Parnavelas JG, Stumm R. CXC chemokine receptor 7 (CXCR7) affects the migration of GnRH neurons by regulating CXCL12 availability. *J Neurosci*. 2013;33:17527–17537. doi: 10.1523/JNEUROSCI.0857-13.2013.
42. Hahner S, Stuermer A, Kreissl M, Reiners C, Fassnacht M, Haenscheid H, Beuschlein F, Zink M, Lang K, Allolio B, Schirbel A. [123 I] Iodometomidate for molecular imaging of adrenocortical cytochrome P450 family 11B enzymes. *J Clin Endocrinol Metab*. 2008;93:2358–2365. doi: 10.1210/jc.2008-0050.
43. Powlson AS, Gurnell M, Brown MJ. Nuclear imaging in the diagnosis of primary aldosteronism. *Curr Opin Endocrinol Diabetes Obes*. 2015;22:150–156. doi: 10.1097/MED.0000000000000148.
44. Burton TJ, Mackenzie IS, Balan K, Koo B, Bird N, Soloviev DV, Azizan EA, Aigbirhio F, Gurnell M, Brown MJ. Evaluation of the sensitivity and specificity of (11)C-metomidate positron emission tomography

- (PET)-CT for lateralizing aldosterone secretion by Conn's adenomas. *J Clin Endocrinol Metab.* 2012;97:100–109. doi: 10.1210/jc.2011-1537.
45. Hahner S, Kreissl MC, Fassnacht M, Haenscheid H, Bock S, Verburg FA, Knoedler P, Lang K, Reiners C, Buck AK, Allolio B, Schirbel A. Functional characterization of adrenal lesions using [123I]IMTO-SPECT/CT. *J Clin Endocrinol Metab.* 2013;98:1508–1518. doi: 10.1210/jc.2012-3045.
  46. Hennings J, Lindhe O, Bergström M, Långström B, Sundin A, Hellman P. [11C]metomidate positron emission tomography of adrenocortical tumors in correlation with histopathological findings. *J Clin Endocrinol Metab.* 2006;91:1410–1414. doi: 10.1210/jc.2005-2273.
  47. Reincke M, Beuschlein F, Latronico AC, Arlt W, Chrousos GP, Allolio B. Expression of adrenocorticotrophic hormone receptor mRNA in human adrenocortical neoplasms: correlation with P450scc expression. *Clin Endocrinol (Oxf).* 1997;46:619–626.
  48. Bluemel C, Hahner S, Heinze B, Fassnacht M, Kroiss M, Bley TA, Wester HJ, Kropf S, Lapa C, Schirbel A, Buck AK, Herrmann K. Investigating the chemokine receptor 4 as potential theranostic target in adrenocortical cancer patients. *Clin Nucl Med.* 2017;42:e29–e34. doi: 10.1097/RLU.0000000000001435.
  49. Soret M, Bacharach SL, Buvat I. Partial-volume effect in PET tumor imaging. *J Nucl Med.* 2007;48:932–945. doi: 10.2967/jnumed.106.035774.

## Novelty and Significance

### What Is New?

- CXCR4 (CXC chemokine receptor type 4) is highly expressed in the outer adrenocortical zones, as well as in aldosterone-producing adenomas, especially compared with nonfunctioning adenomas.
- The CXCR4-specific positron emission tomographic tracer 68Ga-pentixafor exhibits strong binding to cryosections of aldosterone-producing adenomas, adrenocortical carcinomas, and the outer adrenal cortex.
- First in vivo imaging studies show the potential suitability of CXCR4-specific positron emission tomographic imaging for noninvasive subtype differentiation in patients with primary aldosteronism.

### What Is Relevant?

- Alternative tools for subtype differentiation in primary aldosteronism are urgently needed because of several drawbacks of the current diagnostic

standard adrenal vein sampling. Given the high expression of CXCR4, especially in aldosterone-producing adenomas, as well as strong tracer binding of 68Ga-pentixafor to aldosterone-producing adenomas, CXCR4 seems to be a suitable target for noninvasive characterization of adrenal lesions in primary aldosteronism.

### Summary

CXCR4-targeted positron emission tomographic imaging represents a novel promising alternative to adrenal vein sampling for differential diagnosis in primary aldosteronism.

## Targeting CXCR4 (CXC Chemokine Receptor Type 4) for Molecular Imaging of Aldosterone-Producing Adenoma

Britta Heinze, Carmina T. Fuss, Paolo Mulatero, Felix Beuschlein, Martin Reincke, Mona Mustafa, Andreas Schirbel, Timo Deutschbein, Tracy Ann Williams, Yara Rhayem, Marcus Quinkler, Nada Rayes, Silvia Monticone, Vanessa Wild, Celso E. Gomez-Sanchez, Anna-Carina Reis, Stephan Petersenn, Hans-Juergen Wester, Saskia Kropf, Martin Fassnacht, Katharina Lang, Ken Herrmann, Andreas K. Buck, Christina Bluemel and Stefanie Hahner

*Hypertension*. 2018;71:317-325; originally published online December 26, 2017;

doi: 10.1161/HYPERTENSIONAHA.117.09975

*Hypertension* is published by the American Heart Association, 7272 Greenville Avenue, Dallas, TX 75231

Copyright © 2017 American Heart Association, Inc. All rights reserved.

Print ISSN: 0194-911X. Online ISSN: 1524-4563

The online version of this article, along with updated information and services, is located on the World Wide Web at:

<http://hyper.ahajournals.org/content/71/2/317>

Data Supplement (unedited) at:

<http://hyper.ahajournals.org/content/suppl/2017/12/22/HYPERTENSIONAHA.117.09975.DC1>

**Permissions:** Requests for permissions to reproduce figures, tables, or portions of articles originally published in *Hypertension* can be obtained via RightsLink, a service of the Copyright Clearance Center, not the Editorial Office. Once the online version of the published article for which permission is being requested is located, click Request Permissions in the middle column of the Web page under Services. Further information about this process is available in the [Permissions and Rights Question and Answer](#) document.

**Reprints:** Information about reprints can be found online at:

<http://www.lww.com/reprints>

**Subscriptions:** Information about subscribing to *Hypertension* is online at:

<http://hyper.ahajournals.org/subscriptions/>



## ONLINE SUPPLEMENT

### TARGETING CHEMOKINE RECEPTOR CXCR4 FOR MOLECULAR IMAGING OF ALDOSTERONE-PRODUCING ADENOMA

Britta Heinze<sup>1\*</sup>, Carmina T. Fuss<sup>1\*</sup>, Paolo Mulatero<sup>2</sup>, Felix Beuschlein<sup>3</sup>, Martin Reincke<sup>3</sup>, Mona Mustafa<sup>4</sup>, Andreas Schirbel<sup>5</sup>, Timo Deutschbein<sup>6</sup>, Tracy Ann Williams<sup>2,3</sup>, Yara Rhayem<sup>3</sup>, Marcus Quinkler<sup>7</sup>, Nada Rayes<sup>8</sup>, Silvia Monticone<sup>2</sup>, Vanessa Wild<sup>9</sup>, Celso E. Gomez-Sanchez<sup>10</sup>, Anna-Carina Reis<sup>11</sup>, Stephan Petersenn<sup>12</sup>, Hans-Juergen Wester<sup>13</sup>, Saskia Kropf<sup>14</sup>, Martin Fassnacht<sup>1,6</sup>, Katharina Lang<sup>1</sup>, Ken Herrmann<sup>5</sup>, Andreas K. Buck<sup>5</sup>, Christina Bluemel<sup>5</sup>, Stefanie Hahner<sup>1</sup>

\*equal contribution

1 Endocrinology & Diabetes Unit, Department of Internal Medicine I, University Hospital of Wuerzburg, University of Wuerzburg, Germany;

2 Division of Internal Medicine and Hypertension, Department of Medical Sciences, University of Torino, Italy;

3 Medizinische Klinik und Poliklinik IV, Klinikum der Universität München, Germany,

4 Department of Nuclear Medicine, Klinikum rechts der Isar der Technischen Universität München, Munich, Germany

5 Department of Nuclear Medicine, University Hospital of Wuerzburg, University of Wuerzburg, Germany;

6 Comprehensive Cancer Center Wuerzburg, University Hospital of Wuerzburg, University of Wuerzburg, Germany

7 Endocrinology in Charlottenburg, Berlin, Germany.

8 Department of General, Visceral, and Transplant Surgery, Charité - Universitätsmedizin Berlin, Campus Virchow Klinikum, Berlin, Germany

9 Department of Pathology, University Hospital Würzburg, Germany;

10 Division of Endocrinology, G.V. (Sonny) Montgomery VA Medical Center Mississippi, USA;

11 Institute of Pathology, University Hospital Essen, University of Duisburg-Essen, Germany;

12 ENDOC, Center for Endocrine Tumors, Hamburg, Germany

13 Pharmaceutical Radiochemistry, Technische Universität München , 85748 Garching, Germany

14 SCINTOMICS GmbH, Lindach 4, 82256 Fürstenfeldbruck, Germany

Short title: CXCR4 expression in aldosterone-producing adenoma

Correspondence:

Stefanie Hahner, MD, Endocrinology & Diabetes Unit, Department of Medicine I, University of Wuerzburg, Oberduerrbacher Str. 6, D-97080 Wuerzburg, Germany, Fax: 0049-931-201-639200, Phone: 0049-931-201-39200, e-mail: hahner\_s@ukw.de

## MATERIALS AND METHODS

### Immunohistochemical analysis

As a screening test for primary aldosteronism the aldosterone / renin concentration ratio (ARR) after withdrawal of interfering drugs had been used and diagnosis of PA had subsequently been confirmed by saline infusion test. After confirmation of PA, 103 out of 117 patients underwent adrenal vein sampling. In the remaining 14 patients the decision for adrenalectomy had been based on detection of an adrenal lesion in conventional adrenal imaging combined with younger age (below 45 years) and/or positive postural test. After adrenalectomy, surgical specimens underwent histopathological evaluation by a local pathologist. Unilateral disease was confirmed by normalization of ARR and potassium levels as well as cure or amelioration of hypertension at follow-up (available for 113/117 patients). All patients with cortisol producing adenoma had an abnormal dexamethasone suppression test defined as serum-cortisol level after 1 mg dexamethasone above 1.8 µg/dl. Mean serum cortisol levels after dexamethasone were 15.9 µg/dl (2.2 – 30.6 µg/dl). In addition, at least one further pathological test of the HPA axis was required for inclusion as CPA: 24 hour urine cortisol levels above the normal range and increased salivary or serum cortisol levels at midnight.

Patients with non-functioning adrenocortical adenoma had no clinical evidence of hormone excess and furthermore normal tests results for aldosterone to renin ratio and cortisol levels. The respective local specialists of the departments of pathology confirmed histological diagnosis of adrenocortical adenoma.

Tissue sections were deparaffinized in xylene for 2x12 min and dehydrated in ethanol (100%, 90%, 80%, 70%, each concentration for 5 min). Immunohistochemical detection was performed using an indirect immunoperoxidase technique after high temperature antigen retrieval in 10 mM citric acid monohydrate buffer (pH 6.5) in a pressure cooker for 13 min. Blocking of unspecific protein-antibody interactions was performed with 20% human AB-serum in PBS for 1 hour at room temperature. The primary CXCR4 antibody was used at a dilution of 1:100 at RT for 1 h together with the N-Universal Negative Control Anti-Rabbit (Dako, Glostrup, Denmark). CXCR4 and CXCL12 antibodies were from abcam (Cambridge, United Kingdom (12824, 9797)) Specific antibodies against human CYP11B1 (dilution 1:100) and CYP11B2 (dilution 1:200) were kindly provided by Celso Gomez-Sanchez, University of Mississippi, USA. Signal amplification was achieved by En-Vision System Labeled Polymer-Horseradish peroxidase (Dako, Santa Clara, USA) for 40 min and developed for 10 min with Diaminobenzidine Substrate Kit (Vector Laboratories, Burlingame, CA, USA) according to the manufacturer's instructions. Nuclei were counterstained with Mayer's hematoxylin for 2 min. Negative controls were carried out by treating the slides with a nonimmune serum instead of the primary antibody, yielding a nearly complete loss of staining with only some faint background.

The anti-CXCR4, anti-CYP11B2 and anti-CYP11B1 staining intensity was evaluated with a grading score of 0, 1, 2, or 3, which corresponded to negative, weak, moderate, or strong staining intensity, respectively. The percentage of positive tumor cells was calculated for each specimen and scored 0 if 0% were positive, 0.1 if 1–9%, 0.5 if 10–49%, and 1 if >50%. A semi-quantitative h-score was then calculated by multiplying the staining intensity grading score with the proportion score as previously described<sup>1</sup>. Calculation of h-score was separately performed for membrane and cytoplasmatic staining in tumor tissue as well as the adjacent adrenal gland. For membrane and cytoplasmatic staining an h-score ≤ 1 was rated as

low, whereas and h-score > 1 was rated as high. Investigators were blinded to the patient data.

#### Analysis of chemokine receptor expression in adrenocortical adenomas by quantitative PCR

40 ng cDNA was used for each PCR reaction and each sample was performed in duplicate. Transcript levels were determined using the TaqMan Gene Expression Master Mix (Applied Biosystems, Foster City, USA), the CFX96 real-time thermocycler (Bio-Rad, Hercules, CA, USA) and Bio-Rad CFX Manager 2.0 software. Cycling conditions were 95°C for three min followed by 50 cycles of 95°C for 30 sec, 60°C for 30 sec, and 72°C for 30 sec. Using the  $\Delta\text{CT}$  method<sup>2</sup>, the gene expression levels were normalized to those of b-actin.

#### Autoradiographic experiments with 68Ga-Pentixafor

Human tissues were snap-frozen in liquid nitrogen to block further biological processes including protein degradation and tissue hardening and stored at -80 °C. Experiments were repeated thrice. Before cutting, tissues were transferred to a -20 °C freezer. Frozen samples were sectioned in a micro-cryotome into 20 µm tissue slices for all tissues and thaw-mounted onto superfrost slides, dried and then stored at -80 °C until processing. A barrier pen was used (Invitrogen Mini PAP PEN, Zymed® Laboratories, Carlsbad, CA, USA). For the experimental set-up the tissue slices were fixated for 10 min with 0.4%PFA and then pre-incubated for 5 min at room temperature with buffer solution (pH 7.4, 50 mM Tris). Afterwards the slices were incubated with 20% human AB-serum in PBS for 60 min. After blocking for 1 hour, one slide was treated with 2 MBq 68Ga-Pentixafor and another slide was incubated with 2 MBq 68Ga-Pentixafor plus 10 µM of the non-radioactive compound to monitor the specific binding. Slides were subsequently washed twice in 0.5% Tween 50 mM Tris HCl buffer solution (pH 7.4) and dried. Thereafter, samples were placed for 30 min on Phosphor Imager plates in dedicated lead shielded cassettes. Autoradiographic images were analyzed with a Phosphor Imager (CR35BIO Imageplate scanner) and data analysis was performed with Amide software Version 0.9.0 and Microsoft Excel® 2007.

#### Imaging of patients by 68Ga-Pentixafor-PET

In the four patients receiving PET/CT, corresponding CT low dose scans for attenuation correction were acquired using a low-dose protocol (20 mAs, 120keV, a 512x512 matrix, 5mm slice thickness, increment of 30mm/s, rotation time of 0.5s, and pitch index of 0.8) including the base of the skull to the proximal thighs for the reference group and including one bed position over the abdomen for the patients with primary aldosteronism. Consecutively, PET emission data were acquired in three-dimensional mode with a 200x200 matrix with 2-3min emission time per bed position. After decay and scatter correction, PET data were reconstructed iteratively with attenuation correction using a dedicated software (Siemens Esoft).

In the remaining five patients, PET and MR data were simultaneously acquired for 20 min on the integrated PET/MR system 50 to 69 min after injection of 68Ga-Pentixafor. The PET scan was acquired in 3D-list-mode including PET-based respiratory gating, attenuation correction was accomplished using 2-point Dixon MR sequences. For anatomical correlation T1w and T2 fatsat axial sequences, as well as T2w coronal sequences were acquired.

In all cases 68Ga-Pentixafor scans were performed on a dedicated PET/CT (Siemens Biograph mCT 64 and Biograph mCT 128; Siemens Medical Solutions, Erlangen, Germany) or PET/MRI System (Siemens Biograph mMR; Siemens Medical Solutions, Erlangen, Germany). Injected activity ranged from 115 to 207 MBq and image acquisition started after 50 to 86 min.

Semi-quantitative PET scan analysis comprised calculation of the highest metabolic activity within each adrenal gland (maximum standardized uptake values, SUVmax) by 2D regions of interest (ROI) with a diameter of 1 cm around the hottest pixel. CT and MRI scans were read qualitatively by reporting the location and size of adrenal lesions.

68Ga-Pentixafor was administered under the conditions of pharmaceutical law (The German Medicinal Products Act, AMG §13 2b) according to the German law and in accordance with the responsible regulatory body (Regierung von Unterfranken, Regierung von Oberbayern, Germany) <sup>3</sup>. All patients gave written informed consent prior to 68Ga-Pentixafor-PET imaging.

## References

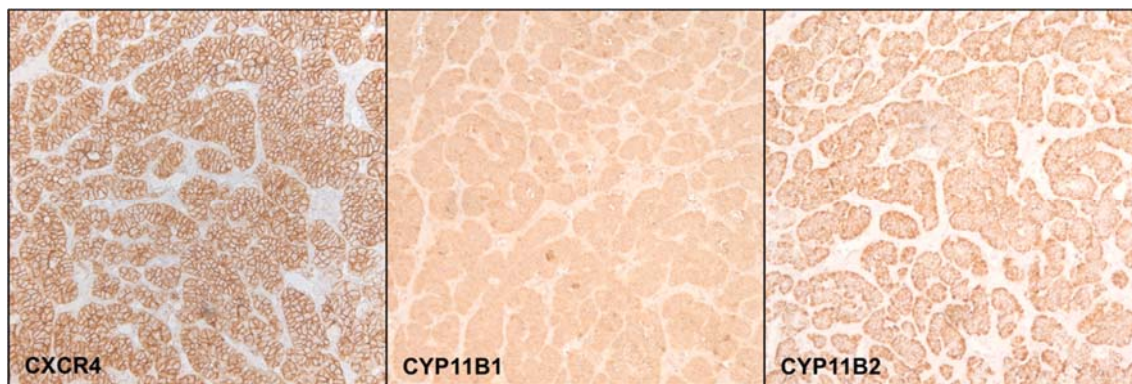
1. Ronchi CL, Sbiera S, Altieri B, Steinhauer S, Wild V, Bekteshi M, Kroiss M, Fassnacht M, Allolio B. Notch1 pathway in adrenocortical carcinomas: Correlations with clinical outcome. *Endocrine-related cancer*. 2015;22:531-543
2. Pfaffl MW. A new mathematical model for relative quantification in real-time rt-pcr. *Nucleic acids research*. 2001;29:e45
3. Haug AR, Cindea-Drimus R, Auernhammer CJ, Reincke M, Beuschlein F, Wangler B, Uebles C, Schmidt GP, Spitzweg C, Bartenstein P, Hacker M. Neuroendocrine tumor recurrence: Diagnosis with 68ga-dotatate pet/ct. *Radiology*. 2014;270:517-525



## Results

| Chemokine<br>Receptor | Taqman Gene<br>Expression assay |
|-----------------------|---------------------------------|
| CCR1                  | Hs00928897_s1                   |
| CCR2                  | Hs00704702_s1                   |
| CCR3                  | Hs01847760_s1                   |
| CCR4                  | Hs00747615_s1                   |
| CCR5                  | Hs99999149_s1                   |
| CCR6                  | Hs10890706_s1                   |
| CCR7                  | Hs01013469_m1                   |
| CCR8                  | Hs00174764_m1                   |
| CCR9                  | Hs01890924_s1                   |
| CCR10                 | Hs00706455_s1                   |
| CCR11                 | Hs00664347_s1                   |
| CXCR1                 | Hs01921207_s1                   |
| CXCR2                 | Hs01891184_s1                   |
| CXCR3                 | Hs01847760_s1                   |
| CXCR4                 | Hs00607978_s1                   |
| CXCR5                 | Hs00540548_s1                   |
| CXCR6                 | Hs01890898_s1                   |
| CXCR7                 | Hs00664172_s1                   |
| b-actin               | Hs9999903_m1                    |

S1. Specific Taqman Gene Expression assays by Applied Biosystems (Darmstadt, Germany).



S2. Immunohistochemical staining of CXCR4, CYP11B1 and CYP11B2 in aldosterone-producing adenoma, Magnification 10x.